de Rooij *et al.*
Journal of Analytical Science and Technology (2023) 14:49
https://doi.org/10.1186/s40543-023-00413-1

Journal of Analytical Science and Technology

TECHNICAL NOTE

Open Access

Quantification of bone surface textures: exploring a new method of ontogenetic ageing

Jimmy de Rooij[1,2*], Marleen Q. Vintges[2,3], Thim Zuidwijk[4], Carel T. H. Heerkens[4] and Anne S. Schulp[1,2]

Abstract

Identification of ontogenetic age classes plays an important role in the fields of zoology, palaeontology and archaeology, where accurate age classifications of (sub)fossil remains are a crucial component for the reconstruction of past life. Textural ageing—the identification of age-related bone surface textures—provides a size-independent method for age assessment of vertebrate material. However, most of the work so far is limited to qualitative results. While qualitative approaches provide helpful insights on textural ageing patterns, they are heavily subject to observer bias and fall short of quantitative data relevant for detailed statistical analyses and cross-comparisons. Here, we present a pilot study on the application of 3D surface digital microscopy to quantify bone surface textures on the long bones of the grey heron (*Ardea cinerea*) and the Canada goose (*Branta canadensis*) using internationally verified roughness parameters. Using a standardised measuring protocol, computed roughness values show a strong correlation with qualitative descriptions of textural patterns. Overall, higher roughness values correspond to increased numbers of grooves and pits and vice versa. Most of the roughness parameters allowed distinguishing between different ontogenetic classes and closely followed the typical sigmoidal animal growth curve. Our results show that bone texture quantification is a feasible approach to identifying ontogenetic age classes.

Keywords Roughness, Surfaces, Taphonomy, Topography, Bone, Ontogeny, Digital microscopy

Introduction

Ontogenetic ageing of fossil vertebrates plays an important role in the reconstruction of the (palaeo)ecology and biological age profiles of (extinct) animal populations. However, the majority of applied methods rely either on the preservation of complete and associated limb bone material or on conducting destructive research to count incremental growth lines inside the bone. Consequently, these strategies may often provide only limited information in archaeological and palaeontological context where fossilised specimens are unique and/or mostly preserved disarticulated and fragmentarily.

Textural ageing of bone surfaces has previously been applied to define a non-destructive size-independent proxy for attained age during lifetime (i.e. ontogenetic age) (Tumarkin-Deratzian et al. 2006). Skeletal elements of specific taxa may develop different types of surface textures during ontogeny. The occurrence of specific texture types is controlled by the network of vascular canals penetrating the bone tissue and opening at the bone surface (Tumarkin-Deratzian et al. 2006). Bones of skeletally immature (i.e. younger) individuals have generally higher growth rates, thus producing a dense vascular network for nutrient transport which translates to increased bone surface roughness (Tumarkin-Deratzian et al. 2006). Contrastingly, skeletally mature individuals do not show active growth which results in relatively smooth bone

*Correspondence:
Jimmy de Rooij
jimmy.derooij@naturalis.nl
[1] Faculty of Geosciences, Utrecht University, Princetonlaan 8A, 3584 CB Utrecht, The Netherlands
[2] Naturalis Biodiversity Center, Darwinweg 2, 2333 CR Leiden, The Netherlands
[3] Faculty of Science, Institute of Biology, Leiden University, Sylviusweg 72, 2333 BE Leiden, The Netherlands
[4] Department of Imaging Physics, Faculty of Applied Sciences, Delft University of Technology, Lorentzweg 1, 2628 CJ Delft, The Netherlands

surface textures. Based on these observations, skeletal elements of specific taxa may show (local) dynamic shifts in surface roughness related to ontogenetic stage (i.e. age). This provides an independent tool for ontogenetic ageing of animal skeletal remains, which can be applied to fragmentary fossils as long as bone surface areas are preserved.

However, almost all available datasets are limited to qualitative analyses, relying on categorical classes and descriptive terms to define changes in bone surface roughness. The phenomenon of age-related changes in bone surface roughness has been described in several modern and extinct taxa, including the long bones of a small number of modern birds (Neognathae) (Tumarkin-Deratzian et al. 2006; Acosta Hospitaleche and Picasso 2020; Watanabe 2018), the American alligator (*Alligator mississippiensis*) (Tumarkin-Deratzian et al. 2007) and the long bones as well as the enigmatic parietosquamosal complex of horned dinosaurs (*Centrosaurus, Einiosaurus* and *Pachyrhinosaurus*) (Brown et al. 2009; Sampson et al. 1997; Tumarkin-Deratzian 2009, 2010). In addition, a single unpublished thesis project documented ontogenetic changes in bone textural patterns in modern post-Medieval humans (Wijngaarden 2021). While these attempts have successfully established a classification scheme, the qualitative data makes it difficult to conduct detailed statistical analyses. Moreover, this precludes reliable comparisons without introducing observer errors. Only a handful of comparable studies attempted to quantify surface roughness on prehistoric material including bone weathering and erosion stages (i.e. aspects of taphonomy) (Vietti 2016) and assessment of bone tool wear patterns in archaeology (Martisius et al. 2020).

Here we apply digital microscopy to test whether bone surface roughness can be quantified in the context of ontogenetic ageing, using verified roughness parameters in surface metrology. As taphonomic processes such as long-term erosion and weathering damage may significantly compromise the bone surface texture on fossil specimens, our dataset focusses first on modern taxa of which textural ageing patterns have already been established in previous studies (Tumarkin-Deratzian et al. 2006; Watanabe 2018). This will allow for an accurate test of the quantification method without overprinting effects from taphonomy. Comparing the relation between roughness parameters and ontogeny for qualitative and quantitative datasets helps create a baseline for standardisation of quantitative textural ageing methods.

Material and methods

Digital microscopy

A Keyence VHX-6000 digital microscope housed at the Department of Imaging Physics, Faculty of Applied Sciences of the Delft University of Technology was used for the analysis of bone surface roughness. This setup allows for high resolution 2D and 3D measurements to register small variations in surface topography. We performed roughness analyses by quantifying 2D and 3D surface topography following ISO 4287 and ISO 25178 standards, respectively. While these ISO standards provide a wide range of parameters quantifying surface textures, we chose to focus on the commonly applied roughness parameters including the 'average roughness' ('Ra' for 2D surfaces and 'Sa' for 3D surfaces). Ra and Sa values are calculated as the arithmetical mean deviation of valleys and peaks in a measured surface profile. Higher Ra/Sa values correspond to more pronounced valleys and peaks, and thus a rougher surface topography. Likewise, we incorporate peak (Rp) and valley (Rv) heights as well as their difference (Rz) when analysing the different roughness patterns to provide an accurate quantification of bone surface roughness (see Additional file 1).

Specimen selection

Roughness analyses were performed on the humeri, femora and tibiotarsi (i.e. the upper arm bones, thighbones and shinbone, respectively) of the grey heron (*Ardea cinerea)* and the Canada goose (*Branta canadensis*) as the long bones of these taxa are known to show age-related shifts in bone surface texture (Tumarkin-Deratzian et al. 2006; Watanabe and Matsuoka 2013). Moreover, these taxa show insignificant sexual dimorphism that otherwise could influence ontogenetic growth patterns. All individuals of both taxa belong to local populations located in the Netherlands, thus any inter- or intraspecific variation introduced due to mixing of different populations is not expected. Specimens of *Branta canadensis* were collected from independent hunting organisations responsible for population control. As these specimens were mainly acquired through targeted culling, they exclusively represent skeletally mature individuals. The restricted ontogenetic classes of the *B. canadensis* samples provide an ideal dataset to evaluate the consistency and robustness of the applied techniques tested here. Specimens of *Ardea cinerea* were housed at the natural history museum of Rotterdam, the Netherlands, and were field collected after natural death. The heron specimens represent an ontogenetic series of differently sized individuals (Fig. 1). Individual birds were dissected and the left and right humeri, femora and tibiotarsi were removed and subsequently macerated. Maceration entails the removal of organic soft tissue through controlled putrefaction/decomposition in a closed container. As such, this approach allows for the extraction of bones

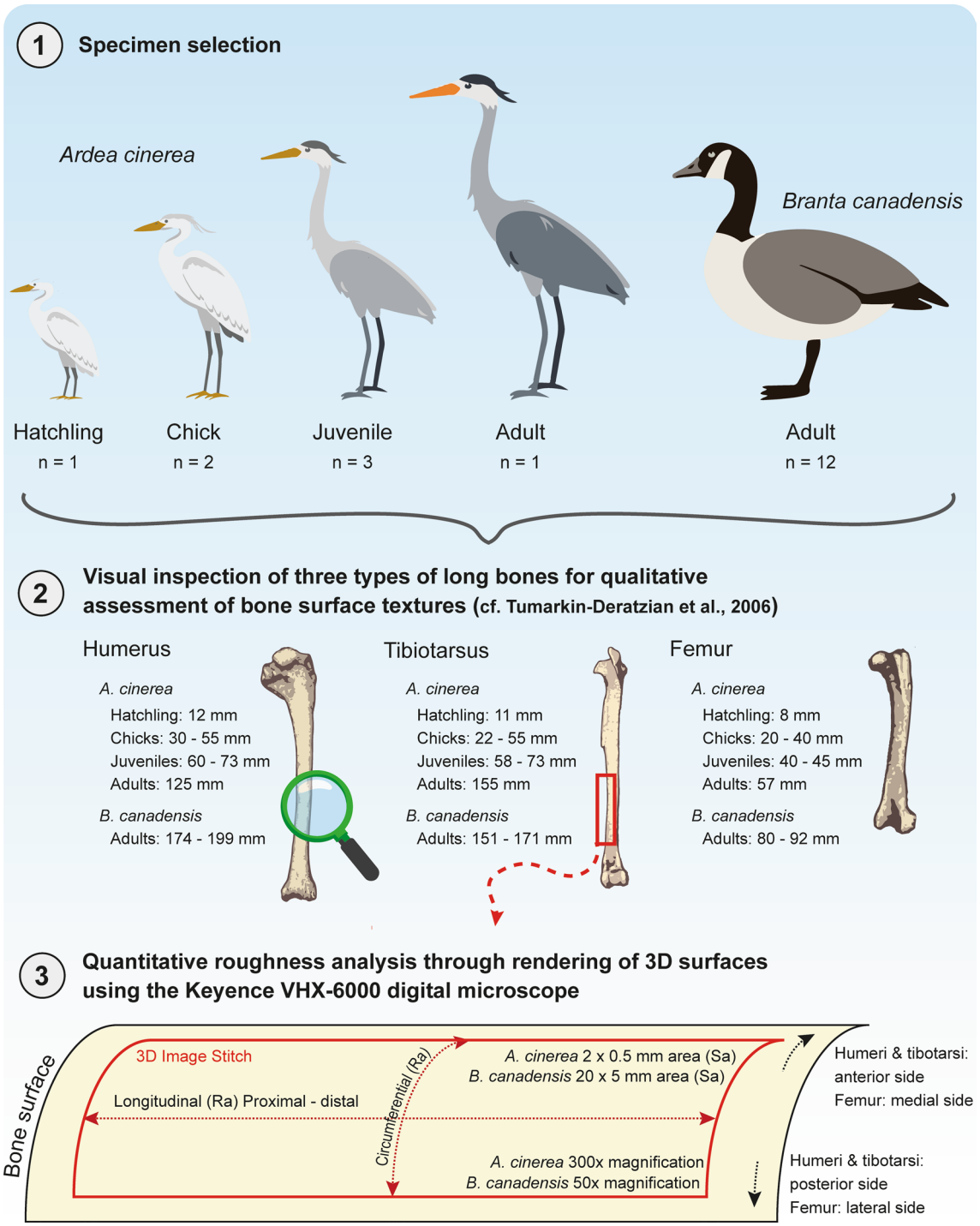

Fig. 1 Overview of the material and methods used in this study. Firstly, relevant taxa and their ontogenetic stages were chosen for sampling. The humeri, tibiotarsi and femora were removed and processed. After a qualitative analysis, each bone was studied using digital microscopy yielding quantitative roughness values. The measurement values in section "Material and methods" indicate the size range of each corresponding sampled bone for all four ontogenetic classes for both taxa

without compromising bone surfaces through potential cut marks.

Measuring protocol

Figure 1 shows a complete overview of the research protocol. Firstly, a qualitative assessment using visual images of the bone textural patterns acquired through the Keyence VHX-6000 (equipped with the VH-ZST 20× to 2000× objective) was made for both taxa following similar strategies applied in the literature. The microscope photographs allowed for comparison with the quantitative data. Using the microscope, the mid-diaphysis of each bone was analysed to avoid potential confounding effects of attachment sites for joint cartilage as well as possible changes in surface texture due to bone morphogenesis of proximal and distal joints. Additionally, we avoided areas that contained muscle attachment sites. Following these criteria, the surface roughness of the humeri and tibiotarsi were measured on the anterior and posterior mid-diaphysis, and the surface roughness of the femora was measured on the medial and lateral mid-diaphysis. To obtain a representative image of the bone surface for the surface roughness measurements (Sa), we standardised the size of the sampling area for both *Ardea cinerea* and *Branta canadensis*. *Ardea cinerea* limb bones were smaller than those of *Branta canadensis* and the large absolute size differences between ontogenetically different grey heron specimens required standardised proportions of the sampling area on the mid-diaphysis. This resulted in a mid-diaphyseal sampling area of 2 by 0.5 mm at 300× magnification for the grey heron and 20 by 5 mm at 50× magnification for the Canada goose.

We used the analytical tools bundled with the Keyence VHX-6000 microscope to quantify bone surface roughness. Additional file 2: Table S1 provides all the microscope settings, and no specific filters were used during the analysis. A high-resolution 3D image of the bone surface was rendered for each bone using image-stitching under coaxial light. Specific light settings were unique for each specimen, but we experienced that medium light intensity combined with a variable use of polarizing filter is best practise to improve image quality and reduce glare. Depending on the size of the sampled bone, we demarcated the area of interest (2 or 20 mm apart) on the mid-diaphysis using a pencil to provide reference during image acquisition, and a series of images were stitched along the mid-diaphysis until the preferred sampling area was captured. The lowest and highest points of focus were chosen along the Z-axis for the first and last image, respectively, and a 10 µm vertical pitch guaranteed that the entire stitched image was in focus. The slope and convexity were filtered out in the rendered 3D surface image using step-wise corrections associated with the Keyence software to ensure that the observed variations in surface topography were limited to roughness parameters only (Additional file 2: Figure S1). An ISO-verified built-in line (2D) and areal (3D) roughness analysis was then performed across the indicated surface area to acquire roughness data (Additional file 2: Figure S2). To account for possible errors introduced by different sampling directions, we performed the 2D line analysis longitudinally (in the proximal–distal direction) (2 or 20 mm) as well as circumferentially (perpendicular to that direction) (0.5 or 5 mm) on opposite sides for each bone type (Fig. 1). The raw roughness data is found in the Additional file 1.

Results

Grey heron (*Ardea cinerea*)

Qualitative assessment of the bone surface textures of the grey heron revealed similar structures as previously observed for this taxon (Fig. 2) (Watanabe and Matsuoka 2013). All three limb bones show strong shifts in overall surface texture throughout ontogeny. The adult form is characterized by a relatively smooth bone surface that lacks any kind of large pits, pores or grooves, confirming the ontogenetic position as a skeletally mature adult (Fig. 2). On the other hand, heron chicks display the highest roughness based on the higher amounts of relatively large pores and grooves along the mid-diaphyseal surface (Fig. 2).

Visual inspection of juvenile bones shows a roughness intermediate between chicks and adults, where the abundance and depth of grooves and pits significantly start to diminish with ontogeny (Fig. 2). Of note, the heron hatchlings do not conform to the expected trend of increased porosity in younger individuals (Sibly and Brown 2020), and show relatively less roughness than juveniles. Instead, the bone surface shows a larger number of more superficial fine-grained anastomosing grooves (Fig. 2).

Detailed statistical analyses and data exploration are provided in the Additional file 2. Non-parametric paired Mann–Whitney *U* tests as well as Kruskal–Wallis tests did not reveal a significant difference between the applied measuring procedures for *Ardea cinerea*. In other words, neither the bone area (e.g. anterior or posterior) nor the measuring direction (longitudinal or circumferential) influenced the roughness parameters, and both strategies produced similar data (Additional file 2: Table S2 and S3). Additionally, we found very limited effects of bone type (humeri, tibiotarsi, femora) on roughness values across the studied bird specimens (Additional file 2: Table S5). Thus, considering the major overlap in roughness values within individual birds, we opted to calculate the average values for each roughness parameter and use

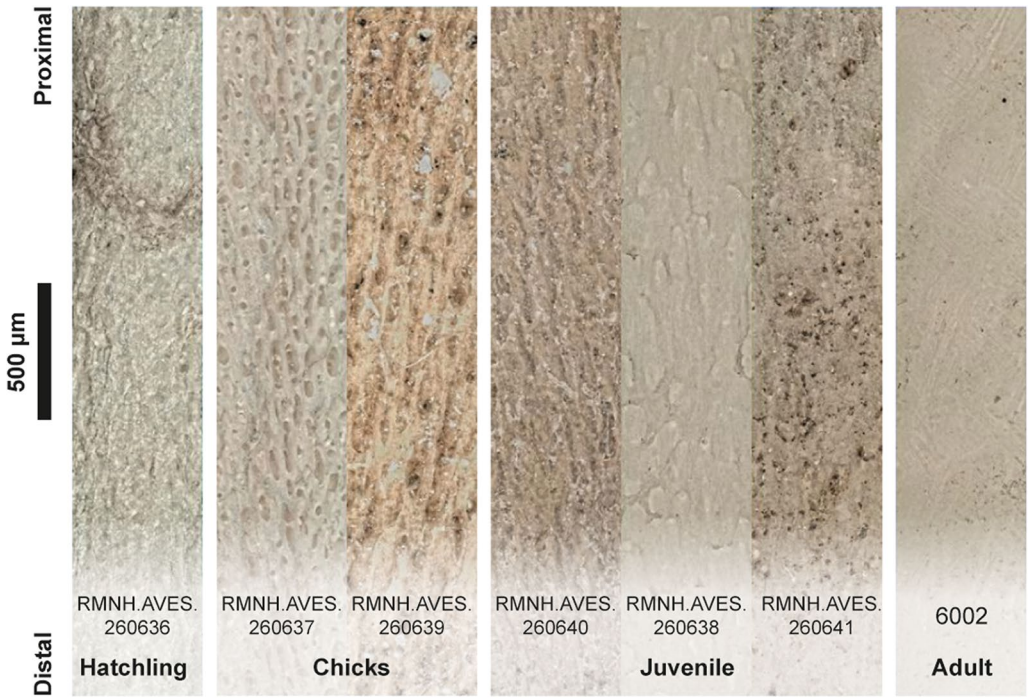

Fig. 2 Qualitative roughness data for *Ardea cinerea* of different ontogenetic stage. Images are from the tibiotarsi, and are taken along the bone's long axis in distal to proximal direction. Chicks show the highest number of large and deep grooves and pits. Hatchlings and juveniles show clear roughness patterns, but only very few penetrating pores. Adults are almost completely smooth

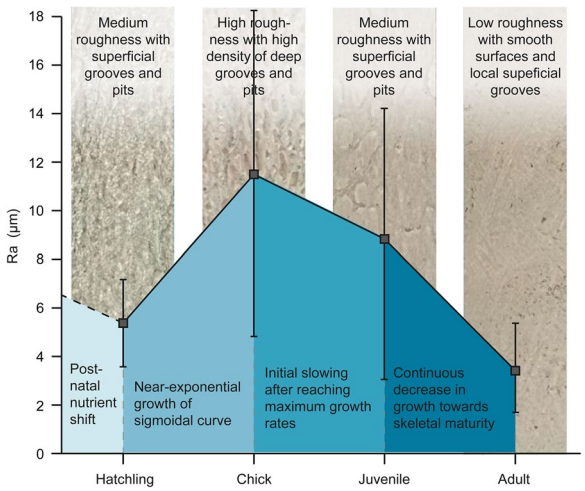

Fig. 3 Relationship between roughness (Ra) and ontogenetic stage. The observed qualitative roughness patterns are positively correlated with the Ra values, and coincide with the proposed shifts in growth rate known for modern birds. The dashed line corresponding to the post-natal nutrient shift is hypothetical. The error bars represent 2σ and show relatively high ranges most likely due to the chosen ontogenetic classes still containing relatively variable roughness values (especially the intermediate classes such as chicks and juveniles, see Discussion)

those for data interpretation and discussion (Additional file 2: Table S6). Figure 3 shows the relationship between average Ra values and ontogenetic age. Similar trends are observed in almost all other roughness parameters including Rv, Rp and Rz (Fig. 4). A paired t-test ($p < 0.05$) shows that Rv values are greater than Rp values for *Ardea cinerea* specimens (See Additional file 2, $p = 0.01$). Ra and Sa values are significantly different ($p = 0.03$), but they show similar relationships with ontogenetic age (Fig. 4). Overall, the roughness parameters all show a predictable pattern that decreases with ontogenetic age, and are in agreement with the qualitative data. Chicks have the highest average Ra (11.5 µm) and adults the lowest (3.4 µm). Hatchlings and juveniles both have intermediate Ra values (5.4 and 8.8 µm, respectively).

Canada goose (*Branta canadensis*)

The ontogenetically restricted *Branta canadensis* samples allow testing of the robustness of bone surface quantification through digital microscopy by repeated measurements of limited ontogenetic age classes. The qualitative assessment of the *Branta canadensis* specimens show very little variation in bone surface textures, corroborating the ontogenetically restricted sample size (Fig. 6A).

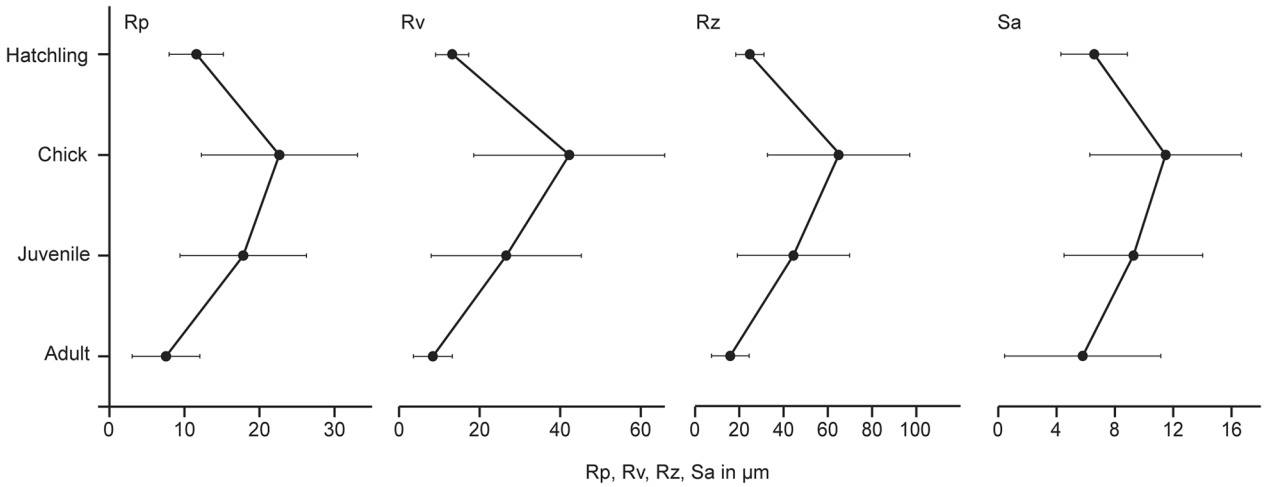

Fig. 4 Relationship between Rp, Rv, Rz, Sa and ontogenetic stage for *Ardea cinerea*. All other major roughness parameters show similar trends as seen in Ra. The error bars represent 2σ

Bone surfaces are all relatively smooth, with only minor local variations in size and abundance of grooves and pits across all the studied samples. They most closely resemble the adult specimens of *Ardea cinerea* as well as previously recorded adult *Branta canadensis* (Tumarkin-Deratzian et al. 2006). The quantitative roughness analysis showed significant differences between Ra values obtained through longitudinal and circumferential measuring directions (Additional file 2: Table S2 and S4). The data obtained from circumferential sampling showed greater spread and higher values that were more randomly distributed (Fig. 5). Thus, we only used the roughness values obtained from longitudinal sampling for our data interpretation. When compared with only the longitudinal data, there is no significant difference in Ra values between the three limb bone types ($p = 0.07$, Additional file 2: Table S6). The *Branta canadensis* dataset was limited to adult specimens only, thus we plotted the average (longitudinal only) Ra values per specimen against bone length, as we assumed that bone length was a general indicator for overall body mass and presumably age. We opted for humerus length to represent body size as the humerus shows the highest size ranges and is thus expected to more accurately visualize the relationship

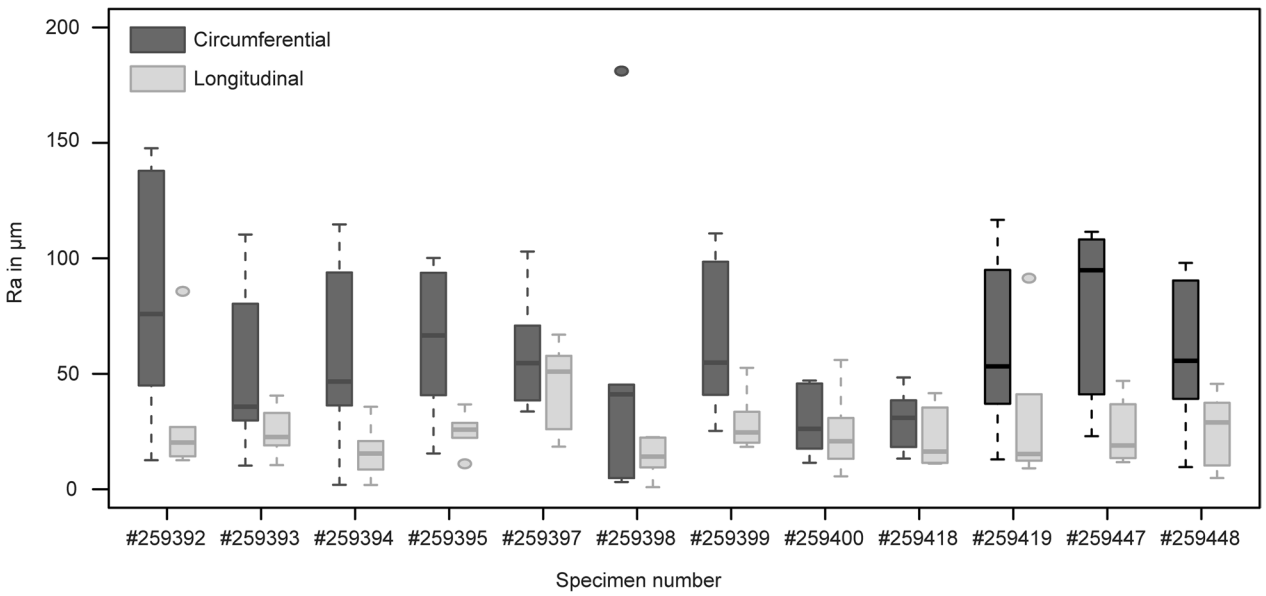

Fig. 5 Comparison between Ra values acquired through longitudinal and circumferential measuring strategies on *Branta canadensis*. Note the consistently higher differences for circumferential data as well as the higher spread

between Ra values and body size. The ontogenetically restricted dataset does not allow for detailed statistical analyses, but the relationship between humerus length and Ra values follow a predictable pattern of decreasing roughness with presumable age (Fig. 6B). Average Ra values per specimen range from 13.9 to 45.2 µm, in which the smallest individual shows the highest Ra value while the largest individual shows the smallest. A paired two sample *t* test ($p < 0.05$) indicates that the Rp values for *Branta canadensis* are significantly larger than the Rv values ($p = 0.00$), and the Rz values are significantly larger than those of *Ardea cinerea* ($p = 0.00$).

Discussion

Comparison of quantitative and qualitative inspection

The general pattern in textural ageing produced through digital microscopy indicates a decrease in surface roughness values with ontogeny. This observed decrease coincides with the loss of superficial grooves and pits during the attainment of skeletal maturity. This pattern is not only observed in the ontogenetic series of *Ardea cinerea* (Figs. 3 and 4), but it even shows within the adult stage of *Branta canadensis* (Fig. 6) where qualitative inspection fails to distinguish the subtle roughness differences. Despite the limited sample sizes, the overlap of both the quantitative and qualitative patterns as well as the consistent output across specimens within both taxa strongly suggest that the digital roughness analyses accurately captured patterns of textural ageing and reflect ontogenetic changes in roughness due to changes in bone vascularity. We do note that the relationship between roughness parameters and ontogenetic stage (Figs. 3 and 4) present relatively large standard deviations, which is most likely a result of the chosen ontogenetic grouping as well as the limited sample sizes. Vertebrate ontogeny is defined by a continuous increase in body size and future attempts should define a broader spectrum of more discrete ontogenetic classes to more accurately document intervals of surface roughness changes during ontogeny. Additionally, the different intrabone measuring strategies compared here revealed little to no effects on the multiple roughness parameters, and where two roughness parameters showed strong significant differences, they still showed similar biological relationships (e.g. Ra and Sa, Figs. 3 and 4).

This work further highlights the importance of following a standardised measuring protocol when analysing quantitative roughness data, at least when using digital microscopy. For example, while most values generated through different measuring strategies showed no appreciable differences, the roughness parameters from longitudinal and circumferential sampling on *Branta canadensis* showed strongly diverging values (Fig. 5). The circumferential measurements resulted in extremely high and scattered Ra values, while in theory these bone surfaces are not expected to show different average roughness within the same area. The current dataset only provides limited explanation on this offset in measuring strategies, but it most likely represents introduced errors as a result of magnification, light intensity and/or post-stitching image transformation and processing. Filtering out the convexity often preserved deformed extremities in the 3D model that overlap with circumferential sampling (e.g. Additional file 2: Figure S1). These confounding

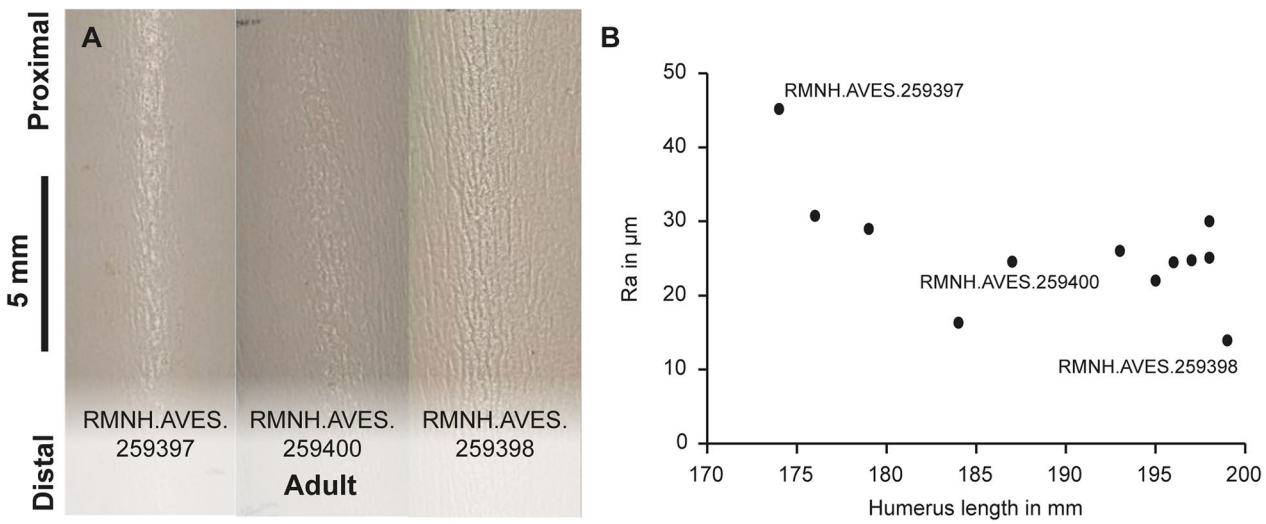

Fig. 6 Qualitative and quantitative roughness data of *Branta canadensis*. **A** Overview of bone textural patterns of the smallest (RMNH.AVES 259397), medium-sized (RMNH.AVES 259400) and largest (RMNH.AVES 259398) specimens. **B** Plot of longitudinally acquired Ra values and associated humerus size. The specimen numbers represent the ones in image **A**. Note the gradual decrease in Ra with larger size

factors do not occur along longitudinal transect parallel to the bone's long axis. As such, following the long axis of long bones produces the most representative roughness values and is considered best practise in our analysis. In addition, the current dataset is too limited to exclude any potential effects of local bone roughness variations within specific age classes. Expansion of the quantitative roughness dataset across local bone areas and more discrete ontogenetic classes should reveal how local bone topography and measuring standards affect roughness values.

Moreover, the strong differences in roughness values between *Ardea cinerea* and *Branta canadensis* also warrants extra scrutiny. Average Ra values of *Branta canadensis* specimens were an order of magnitude higher than *Ardea cinerea*, including ontogenetically younger individuals, despite the qualitative inspection of chick *Ardea cinerea* showing more textured bone surfaces than adult *Branta canadensis*. This most likely represents a measuring artefact introduced by using widely diverging microscope magnifications, as intra-species values acquired using the same magnification still follow the expected ontogenetic trend. Different magnifications may ultimately affect the resolution of the rendered 3D image, thereby potentially altering the threshold of observable microstructures within the surface topography. Thus, our results strongly support a recommendation to use standardised magnifications when examining the same taxon, and care should be taken when comparing multiple taxa.

Ontogenetic changes in bone surface texture

In general, ontogenetically younger animals are expected to show higher growth rates as rapid attainment of adult sizes favours access to limited resources (Sibly and Brown 2020). However, both the qualitative and the quantitative roughness data show the same ontogenetic pattern in which hatchling long bones have a lower roughness compared to the older chick stage. This most likely reflects the typical three phase sigmoidal growth curve of animal development, where initial body mass increases during early ontogeny are relatively low, but increase rapidly during ontogeny after which the growth rate ultimately plateaus (Sibly and Brown 2020; Emmans 2022). The same pattern is observed in the Ra values presented here (Fig. 4) as well as in other parameters including Rv, Rp, Rz and Sa of *Ardea cinerea*. The hatchlings represent the earliest ontogenetic stage after birth, and experience a brief lag phase most likely related to the pre- and postnatal shift in nutrient sources. This corresponds to moderate Ra values, and thus a relatively lower roughness. Subsequently, the higher juvenile Ra values correspond to the extended period of rapid near-exponential growth rates, manifested by increased roughness. Growth rates then significantly decrease again and level off nearing adulthood and skeletal maturity indicated by lower Ra values and smooth surfaces. Similarly, the Ra values for *Branta canadensis* adults still follow the expected trend of decreasing growth rates close to skeletal maturity (Fig. 6). Thus, the close affinity between measured bone surface roughness parameters (e.g. Ra and Sa) and growth rate further corroborates the validity and applicability of quantifying bone textures as conducted in this study.

The data also suggest that *Ardea cinerea* show significantly higher ($p < 0.05$) Rv values (i.e. show deeper valleys) than Rp values ($p = 0.01$). It is reasonable to assume that the blood vessels opening at the bone surface of ontogenetically younger individuals results in deeper grooves creating higher Rv values. Specimens of *Branta canadensis* on the other hand have higher Rp (i.e. higher peaks) than Rv values ($p = 0.00$), which may be a result of sampling a large set of adult specimens that have completely closed bone surfaces creating bone topography mostly defined by peaks. Further analyses on more ontogenically diverse specimens should reveal such patterns more unambiguously.

Implications and future research

This pilot study shows the positive correlation between quantitative roughness data and ontogenetic stage, and provides a foundation and directions for future studies aiming to better quantify and understand patterns in bone surface roughness, with applications in biology, archaeology and palaeontology alike. As data acquisition is completely non-destructive this method may be applied to a large selection of modern and fossil bone material, enabling more thorough collection-based research. As such, it serves as an accurate size-independent proxy for ontogenetic maturity, where it may complement other ageing methods. In order to make this method an established technique, it is necessary to compare qualitative and quantitative bone textural patterns across a larger taxonomic and ontogenetic range. Furthermore, future applications of this technique may help identify to what extent taphonomy (e.g. erosion and weathering) affects the quantitative roughness values (Vietti 2016; Martisius et al. 2020). This enables more accurate identification and ageing of poorly constrained and often fragmentary fossil bones. This way, quantitative surface texture analyses may improve our understanding of aspects of depositional settings and fossil provenance in archaeological and palaeontological context.

Conclusion

The data presented in this pilot study show that quantitative bone surface roughness measurements allow for textural ageing. Preliminary surface topography data following ISO 4287 and 25178 on *Ardea cinerea* and *Branta canadensis* revealed corresponding patterns in ontogenetic shifts between quantitative and qualitative inspection. The Ra, Rv, Rp, Rz and Sa values were positively correlated to the hypothesized changes in growth rate coinciding with the gradual attainment of skeletal maturity. Sampling strategies should adhere to standardised protocols but these can be developed on a case-by-case basis based on the available material as well as taxa. Future research should reveal to what extent the proposed textural ageing method can be applied to the fossil record.

Supplementary Information

The online version contains supplementary material available at https://doi.org/10.1186/s40543-023-00413-1.

Additional file 1. All raw 2D and 3D roughness data sorted per sampling strategy for both *Ardea cinerea* and *Branta canadensis*.

Additional file 2. Statistical analyses of the quantitative roughness data and software output of the Keyence VHX-6000. **Table S1**. Settings of the Keyence VHX-6000 microscope. **Table S2**. Mann-Whitney U tests for roughness data sorted by bone side and measuring directions for *A. cinerea* and *B. canadensis*. **Table S3**. Kruskal-Wallis tests for roughness data sorted by bone side and measuring directions for *A. cinerea*. **Table S4**. Kruskal-Wallis tests for roughness data sorted by bone side and measuring directions for *B. canadensis*. **Table S5**. Kruskal-Wallis tests for roughness data sorted by limb bone per ontogenetic class for *A. cinerea*. **Table S6**. Kruskal-Wallis tests for longitudinal roughness data sorted by limb bone for *B. canadensis*. **Figure S1**. Output of the convexity filter of the Keyence VHX-6000. Output of the 2D roughness analysis of the Keyence VHX-6000.

Acknowledgements

We want to thank Wim van den Assem and Boris Temming for providing us with the *Branta canadensis* specimens and Bram Langeveld and Erwin Kompanje (Natural History Museum Rotterdam, the Netherlands) for access to *Ardea cinerea* specimens. Many thanks to Becky Desjardins (Naturalis, the Netherlands) and Ydnas Louisa for helping with the preparation of the material. We are grateful to Frans Rodenberg (Leiden University, the Netherlands) for his help in setting up the statistical analyses and to Silvania Pereira (Department of Imaging Physics, Delft University of Technology, the Netherlands) for her feedback on the manuscript and discussion on the applied methodology. Lastly, many thanks to the two anonymous reviewers for their time in reading the manuscript and providing comments that improved the manuscript.

Author contributions

JR conceived the initial research plan. MV was responsible for the majority of the analyses conducted for this study. JR, MV, TZ and CH analysed the initial data. JR and MV were major contributors in writing the manuscript as well as data exploration and statistical analyses. More specifically, TZ and CH provided valuable input regarding the material and methods as well as technical support during data acquisition. AS was involved in the study design, and supervised the project. All authors read and approved the final manuscript.

Funding

The project is funded by the Dutch Research Council (NWO) through ALW Open Programme (ALWOP.633).

Availability of data and materials

All data generated and analysed during this study can be found in the 'Supplements Raw Data' file submitted alongside the main text.

Declarations

Competing interests

The authors declare that they have no competing interests.

Received: 1 August 2023 Accepted: 22 November 2023
Published online: 13 December 2023

References

Acosta Hospitaleche C, Picasso MJB. Textural ageing in *Pygoscelis antarctica* (Aves, Sphenisciformes): a new comparative scale for penguin bones. Vertebrate Zoology. 2020;70(2):125–39.

Brown CM, Russell AP, Ryan MJ. Pattern and transition of surficial bone texture of the centrosaurine frill and their ontogenetic and taxonomic implications. J Vertebr Paleontol. 2009;29(1):132–41.

Emmans GC. The potential post-hatching growth of domestic birds is sufficiently described by the Gompertz function. Br Poult Sci. 2022;63(5):701–19.

Martisius NL, McPherron SP, Schulz-Kornas E, Soressi M, Steele TE. A method for the taphonomic assessment of bone tools using 3D surface texture analysis of bone microtopography. Archaeol Anthropol Sci. 2020;12(10):251.

Sampson SD, Ryan MJ, Tanke DH. Craniofacial ontogeny in centrosaurine dinosaurs (Ornithischia: Ceratopsidae): taxonomic and behavioural implications. Zool J Linn Soc. 1997;121(3):293–337.

Sibly RM, Brown JH. Towards a physiological explanation of juvenile growth curves. J Zool. 2020;311(4):286–90.

Tumarkin-Deratzian AR. Evaluation of long bone surface textures as ontogenetic indicators in centrosaurine ceratopsids. Anat Rec. 2009;292(9):1485–500.

Tumarkin-Deratzian AR. Histological evaluation of ontogenetic bone surface texture changes in the frill of *Centrosaurus apertus*. In: Ryan MJ, Chinnery-Allgeier BJ, Ebert DA, editors. New perspectives on horned dinosaurs: the Royal Tyrrell Museum Ceratopsian Symposium. Bloomington: Indiana University Press; 2010. p. 251–63.

Tumarkin-Deratzian AR, Vann DR, Dodson P. Bone surface texture as an ontogenetic indicator in long bones of the Canada goose *Branta canadensis* (Anseriformes: Anatidae). Zool J Linn Soc. 2006;148(2):133–68.

Tumarkin-Deratzian AR, Vann DR, Dodson P. Growth and textural ageing in long bones of the American alligator *Alligator mississippiensis* (Crocodylia: Alligatoridae). Zool J Linn Soc. 2007;150(1):1–39.

Vietti LA. Quantifying bone weathering stages using the average roughness parameter Ra measured from 3D data. Surf Topogr: Metrol Prop. 2016;4(3):034006.

Watanabe J. Ontogeny of surface texture of limb bones in modern aquatic birds and applicability of textural ageing. Anat Rec. 2018;301(6):1026–45.

Watanabe J, Matsuoka H. Ontogenetic change of morphology and surface texture of long bones in the Grey Heron (*Ardea cinerea*, Ardeidae). Paleornithological Research. 2013;(Proceedings of the 8th International Meeting of the Society of Avian Paleontology and Evolution):279–306.

Wijngaarden CL. Bone surface texture and age-at-death of post-Medieval adult skeletal remains from Middenbeemster, the Netherlands: Testing the textural ageing method on human remains. Leiden University, Leiden, MSc Thesis; 2021.

Publisher's Note